Internal Medicine
The Japanese Society of Internal Medicine
doi: 10.2169/internalmedicine.8253-21
Intern Med 61: 2441-2448, 2022
http://internmed.jp

【 CASE REPORT 】

Parietal Cell Dysfunction: A Rare Cause of Gastric Neuroendocrine Neoplasm with Achlorhydria and Extreme Hypergastrinemia

Yasuaki Abe[1], Waku Hatta[1], Sho Asonuma[2], Tomoyuki Koike[1], Hiroko Abe[1], Yohei Ogata[1], Masahiro Saito[1], Xiaoyi Jin[1], Takeshi Kanno[1], Kaname Uno[1], Naoki Asano[1], Akira Imatani[1], Fumiyoshi Fujishima[3], Hironobu Sasano[3] and Atsushi Masamune[1]

Abstract:
A 69-year-old woman with multiple neuroendocrine neoplasms (NENs) was referred to our hospital. Although she had extreme hypergastrinemia (11,675 pg/mL), no findings that indicated types I to III gastric NENs were found. Although gastric corpus atrophy was suspected on conventional white-light imaging, findings on magnifying endoscopy with narrow-band imaging indicated no severe atrophy. A biopsy from the background fundic gland mucosa revealed no atrophic changes, parietal cells with vacuolated cytoplasm and negative findings for H^+K^+-ATPase. Thus, this case was diagnosed as multiple NENs with parietal cell dysfunction. Neither progression nor metastasis has been confirmed during two-year follow-up.

Key words: neuroendocrine neoplasms, parietal cell dysfunction, achlorhydria, hypergastrinemia

(Intern Med 61: 2441-2448, 2022)
(DOI: 10.2169/internalmedicine.8253-21)

Introduction

Gastric neuroendocrine neoplasms (NENs) are classified into three subgroups according to the presence of hypergastrinemia or underlying diseases (1, 2). This classification is useful for determining the treatment strategy for gastric NENs, as these subgroups correlate with metastasis and the prognosis. NENs that do not match the above classification have rarely been reported, and such cases show parietal cell dysfunction in the background mucosa of the stomach.

We herein report a rare case of multiple gastric NENs with parietal cell dysfunction and extreme hypergastrinemia.

Case Report

A 69-year-old Japanese woman with no complaints underwent esophagogastroduodenoscopy (EGD) at a nearby hospital and was found to have multiple elevated gastric lesions diagnosed as NENs by a biopsy. Since it was difficult to diagnose the type of gastric NENs, she was referred to our hospital. She had no history of proton pump inhibitor usage, no history of *Helicobacter pylori* eradication, and no family history of multiple neuroendocrine neoplasia-1 (MEN-1) or other gastric disorders.

Conventional white-light imaging (C-WLI) at our hospital showed 6 yellowish submucosal tumor-like lesions with vasodilation, all of which were <5 mm in maximal diameter, in the fundic gland area of the stomach (Fig. 1A, B). Magnifying endoscopy with narrow-band imaging (ME-NBI) showed an absent microsurface pattern and vasodilation on the top of the tumor (Fig. 1C). The biopsy specimens revealed that the tumor was covered with a monolayer of foveolar epithelium (Fig. 2A), and small nests and cords of polygonal neoplastic cells were present within a fibrotic stroma (Fig. 2B, C). The tumor cells were positive for chromogranin A (Fig. 2D), synaptophysin (Fig. 2E) and CD56 (Fig. 2F). Although atrophic changes in the gastric corpus

[1]Division of Gastroenterology, Tohoku University Graduate School of Medicine, Japan, [2]Department of Gastroenterology, South Miyagi Medical Center, Japan and [3]Department of Pathology, Tohoku University Graduate School of Medicine, Japan
Received: July 1, 2021; Accepted: November 4, 2021; Advance Publication by J-STAGE: February 1, 2022
Correspondence to Dr. Waku Hatta, waku-style@festa.ocn.ne.jp

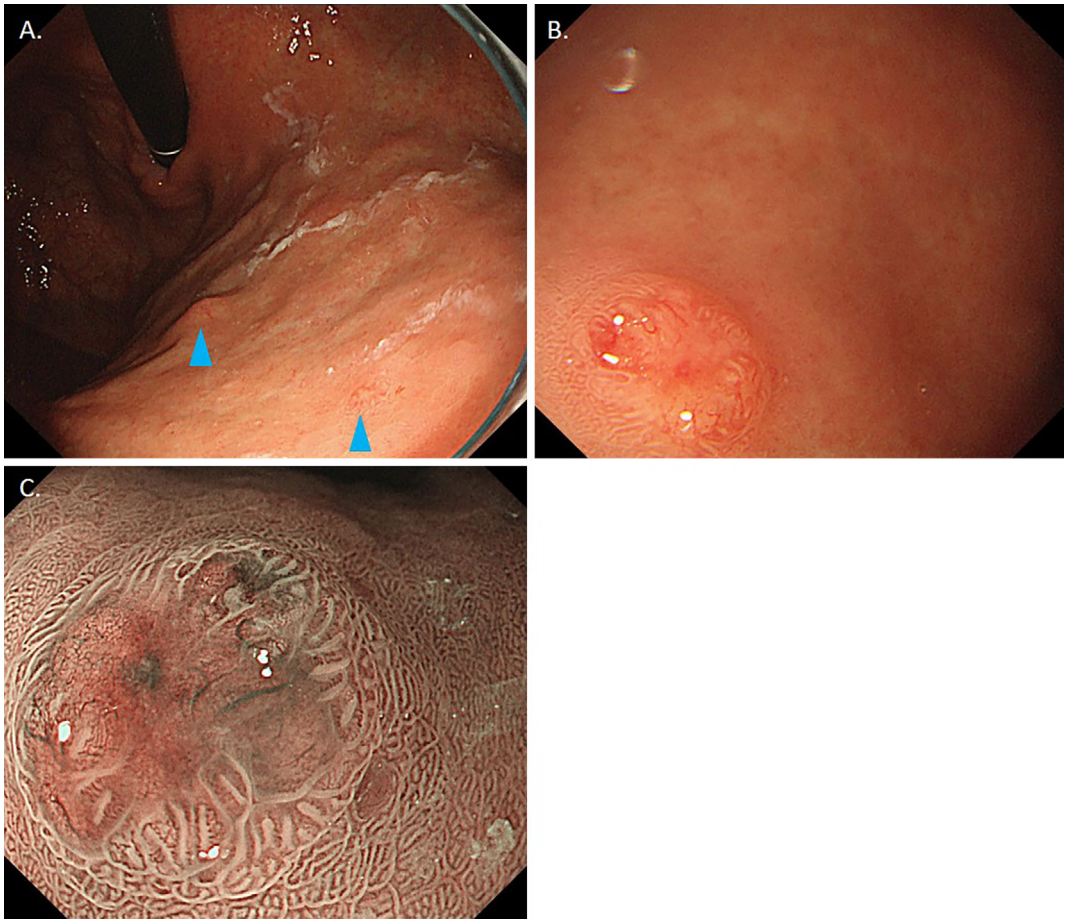

Figure 1. Endoscopic images of gastric NENs. C-WLI showed multiple gastric NENs (light-blue arrows) (A). A NEN located on the greater curvature of the upper body appeared to be a submucosal tumor-like lesion with vasodilation (B). ME-NBI revealed vasodilation and the absence of a microsurface pattern on the top of the tumor (C). NEN: neuroendocrine neoplasm, C-WLI: conventional white-light imaging, ME-NBI: magnifying endoscopy with narrow-band imaging

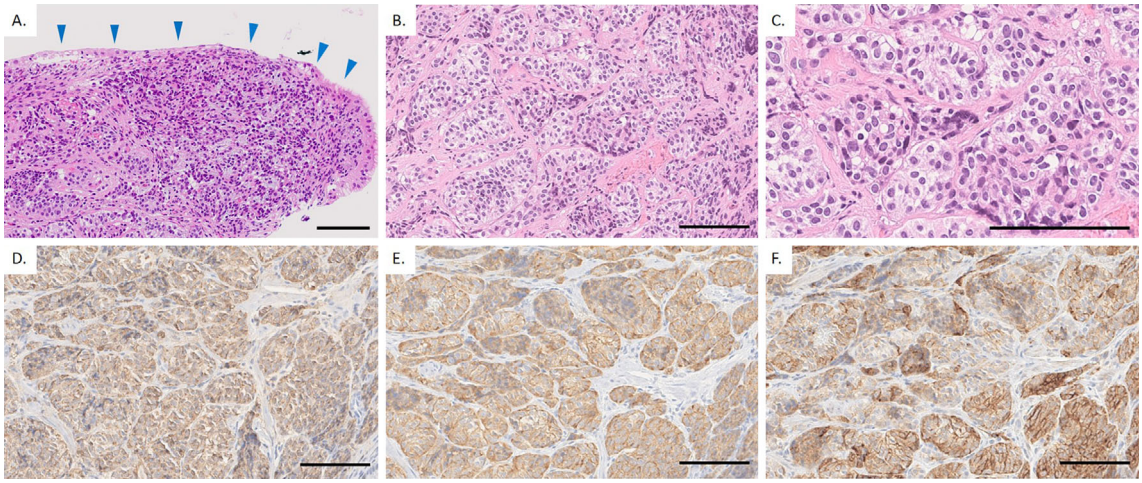

Figure 2. Histopathological findings of a gastric NEN in a biopsy specimen. Hematoxylin and Eosin staining revealed that the tumor was covered with a monolayer of foveolar epithelium (A, blue arrow), and nests and cords of small uniform cuboidal cells were present within a fibrotic stroma (B, C). Immunostaining revealed that the tumor cells were positive for chromogranin A (D), synaptophysin (E) and CD56 (F). Bar=100 μm. NEN: neuroendocrine neoplasm

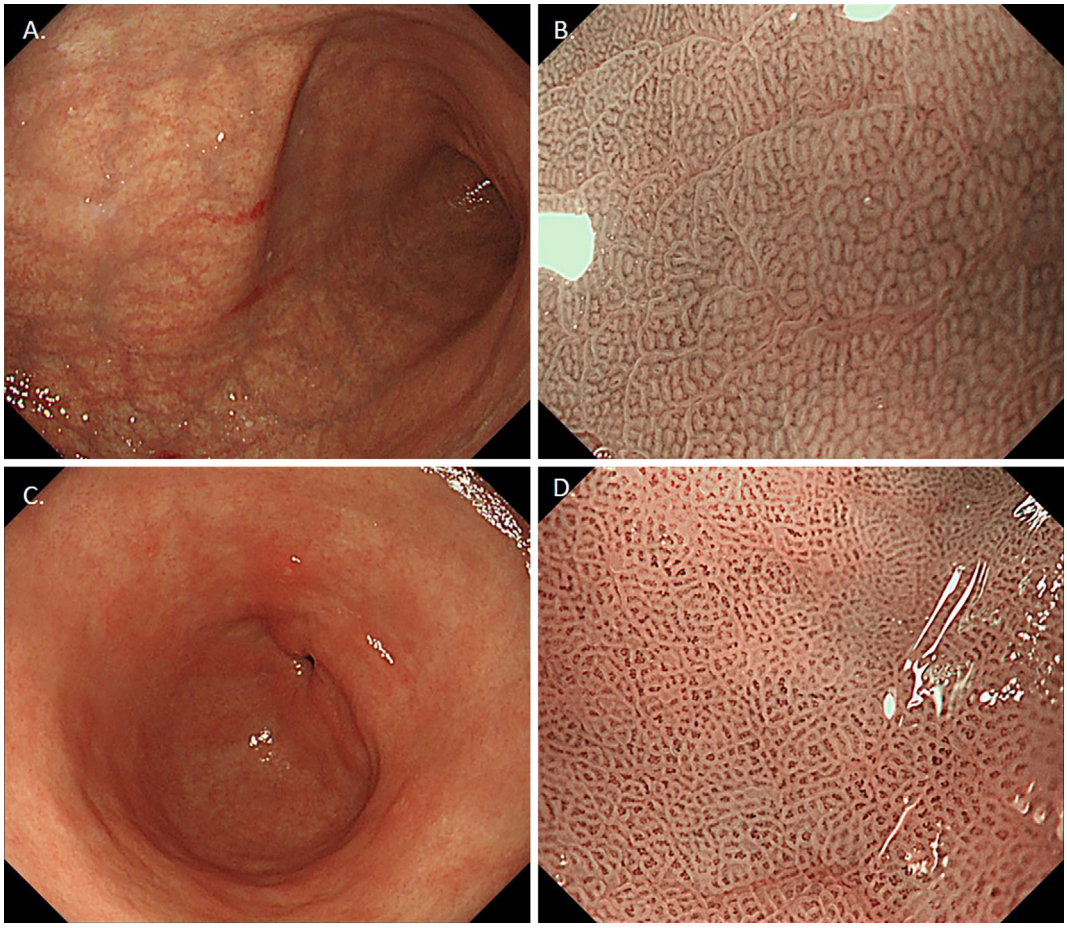

Figure 3. **Endoscopic images of background gastric mucosa. Discolored mucosa with marked vascular visibility on the entire area of the greater curvature of the corpus along with the disappearance of folds without an atrophic border indicated severe atrophic changes in the corpus in C-WLI (A). ME-NBI in the corpus revealed a slightly enlarged, round pit with unclear or irregular subepithelial capillary networks in the corpus (B), indicating the absence of severe gastric atrophy. In the antrum, the visibility of the vascular pattern was negative on C-WLI (C), and subepithelial capillary networks and surrounding circular pits were observed on ME-NBI (D), indicating no atrophy in the gastric antrum. C-WLI: conventional white-light imaging, ME-NBI: magnifying endoscopy with narrow-band imaging**

were suspected on C-WLI, which showed discolored mucosa with vascular visibility on the entire area of the greater curvature of the corpus (Fig. 3A), ME-NBI revealed slightly enlarged, round pits with unclear or irregular subepithelial capillary networks in the corpus (Fig. 3B), suggesting that there may have been no severe gastric atrophy (3, 4). In the antrum, the visibility of the vascular pattern was negative on C-WLI (Fig. 3C), and subepithelial capillary networks and surrounding circular pits were observed on ME-NBI (Fig. 3D), which indicated that there was no atrophy in the gastric antrum (4). No endoscopic findings suggestive of certain diseases, such as enterochromaffin-like (ECL) cell hyperplasia/dysplasia, were observed in the background gastric mucosa.

In the laboratory examination (Table 1), marked hypergastrinemia (11,675 pg/mL) was present; however, no abnormal findings were observed in the titers of serum IgG antibodies against *H. pylori* (*H. pylori*-LATEX "SEIKEN", Denka Ltx, Tokyo, Japan), autoantibodies against intrinsic factor or parietal cell, serum albumin, calcium or intact parathyroid hormone values. *H. pylori* was negative, as also confirmed by the urea breath test (1.6‰). There were no findings suggestive of gastrinoma on computed tomography (CT), somatostatin receptor scintigraphy, selective arterial calcium injection test (Fig. 4) or abdominal angiography. The mean intragastric pH on the 24-hour pH monitoring test was 6.67, indicating a non-acidic condition. We also conducted an endoscopic gastrin test, which estimates the gastrin-stimulated gastric acid secretory response and correlates well with the peak acid output and maximal acid output (5). Although hypochlorhydria and profound hypochlorhydria are defined based on endoscopic gastrin test results of <2.1 and <0.6 mEq/10 min, respectively (6, 7), the value in this case was 0 mEq/10 min, indicating achlorhydria.

An endoscopic biopsy from the endoscopically non-NEN fundic gland mucosa revealed no atrophic changes in the

Table 1. Results of Blood Examination.

	Measured value	Normal range		Measured value	Normal range
WBC	5.2 10^3/μL	3.3-8.6	Ferritin	17.5 ng/mL	12-60
RBC	379 10^4/μL	386-492	Intact PTH	61 pg/mL	10-65
Hb	11.7 g/dL	11.6-14.8	PG I	22.7 ng/mL	>70
Ht	34.7 %	35.1-44.4	PG II	12.2 ng/mL	
PLT	28.1 10^4/μL	15.8-34.8	PG I/II	1.9	>3
TP	7.6 g/dL	6.6-8.1	Vitamin B12	744 pg/mL	180-914
Albumin	4.3 g/dL	4.1-5.1	Folic acid	14.9 ng/mL	≥4.0
Na	139 mmol/L	138-145	Gastrin	11,675 pg/mL	42-200
K	4.6 mmol/L	3.6-4.8	*H. pylori* antibody	<3 U/mL	<3
Cl	102 mmol/L	101-108	Parietal cell antibody	<10	<10
Ca	9.7 mg/dL	8.8-10.1	Intrinsic factor antibody	(-)	(-)

WBC: white blood cell, RBC: red blood cell, Hb: hemoglobin, Ht: hematocrit, PLT: platelet, TP: total protein, Na: sodium, K: potassium, Cl: chlorine, Ca: calcium, PTH: parathyroid hormone, PG: pepsinogen, *H. pylori* antibody: IgG antibody against *Helicobacter pylori*

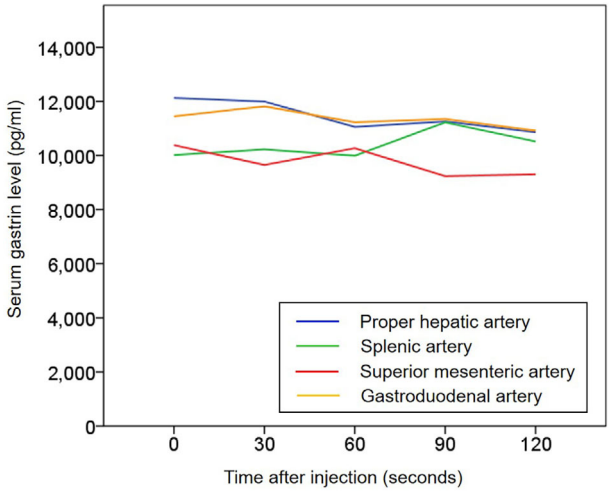

Figure 4. The selective arterial calcium injection test. This test showed no significant increase in the serum gastrin level in any of the evaluated arteries.

fundic gland, but large parietal cells with vacuolated cytoplasm and dilated glands were observed (Fig. 5A, B). The number of parietal cells was not decreased in this case. Although the chief cells were positive for pepsinogen (Fig. 5C), the parietal cells were completely negative for H^+K^+-ATPase (Fig. 5D). Mononuclear cell aggregates were apparent in the deeper mucosa (Fig. 5E), but immunostaining revealed that the number of mononuclear cells positive for CD8 was small (Fig. 5F). The biopsy specimens from the endoscopically non-NEN fundic gland mucosa showed ECL cell hyperplasia/dysplasia around the muscularis mucosa (Fig. 6), which was differentiated from NENs by the fact that an individual nodule was <500 μm (8). In this specimen, parietal cell protrusion was found (Fig. 6A). An endoscopic biopsy from the endoscopically non-NEN antral mucosa showed no intestinal metaplasia or the presence of pyloric glands (Fig. 7). Based on the above findings, the patient was diagnosed with multiple gastric NENs with parietal cell dysfunction.

The mechanism underlying the development of gastric NENs in this type is similar to that in type I gastric NEN (9); thus, the therapeutic approach was decided based on that of type I gastric NEN. According to the guidelines (2), surveillance or endoscopic resection is recommended for type I gastric NEN if the tumor is <1 cm in size, and anterectomy to suppress hypergastrinemia and limit ECL growth is a treatment option. Because all tumors were <5 mm and the patient did not opt for endoscopic resection or anterectomy, follow-up with EGD and CT at 1-year intervals was selected. No progression, metastasis or change in the size or number of gastric NENs has been confirmed during two-year follow-up.

Discussion

Gastric NENs account for 5.6-8.7% of all digestive NENs (10-12), and most cases with gastric NENs are subdivided into three types: type I, gastric NENs that develop against a background of atrophic gastritis (autoimmune gastritis or *H. pylori*-related chronic gastritis) and achlorhydria with hypergastrinemia; type II, gastric NENs that occur in the setting of gastrinoma and hyperchlorhydria that occurs as a part of MEN-1; and type III, gastric NENs that occur sporadically without hypergastrinemia (1, 2). To date, only five cases of gastric NENs associated with parietal cell dysfunction have been reported worldwide (Table 2) (9, 13-15). Vacuolation of parietal cells is a characteristic of parietal cell dysfunction, but it is reported to be associated with long-term proton pump inhibitor use or *H. pylori* infection (16). In the present case, the patient had no history of long-term proton pump inhibitor use, and *H. pylori* findings were negative, with no history of its eradication. Furthermore, parietal cell protrusion and dilated fundic glands with completely negative staining for H^+K^+-ATPase were also observed. We therefore diagnosed this case as a gastric NEN with parietal cell dysfunction, making it the sixth case of such a tumor.

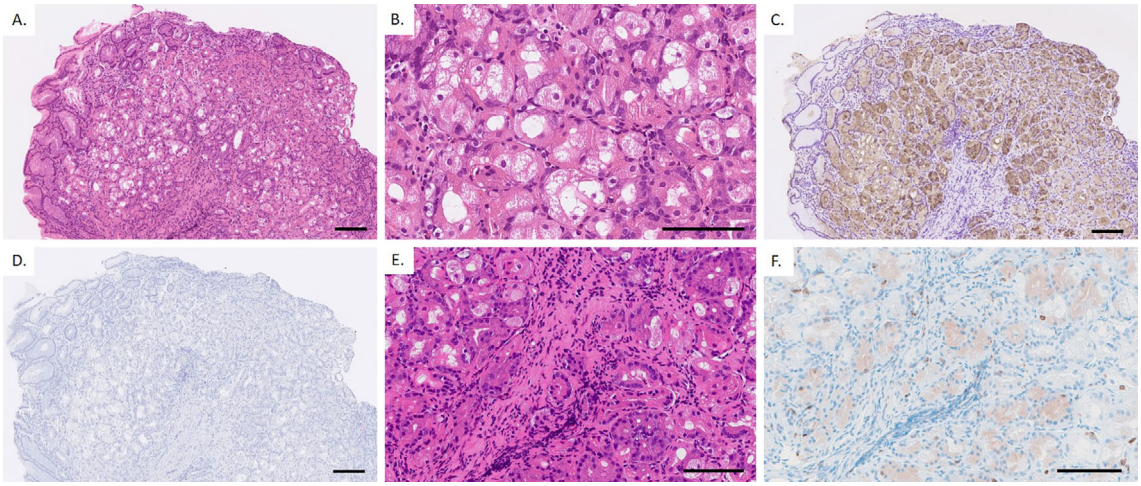

Figure 5. **Histopathological findings of parietal cell dysfunction. Hematoxylin and Eosin staining showed dilated glands and no atrophic change of the fundic glands (A). The parietal cell cytoplasm was vacuolated (B). On immunostaining, the chief cells were positive for pepsinogen (C), but the parietal cells were completely negative for H^+K^+-ATPase (D). In the deeper mucosa, mononuclear cell aggregates were apparent (E). Immunostaining revealed that the number of mononuclear cells positive for CD8 (F) was small, indicating very mild inflammation. Bar=100 μm.**

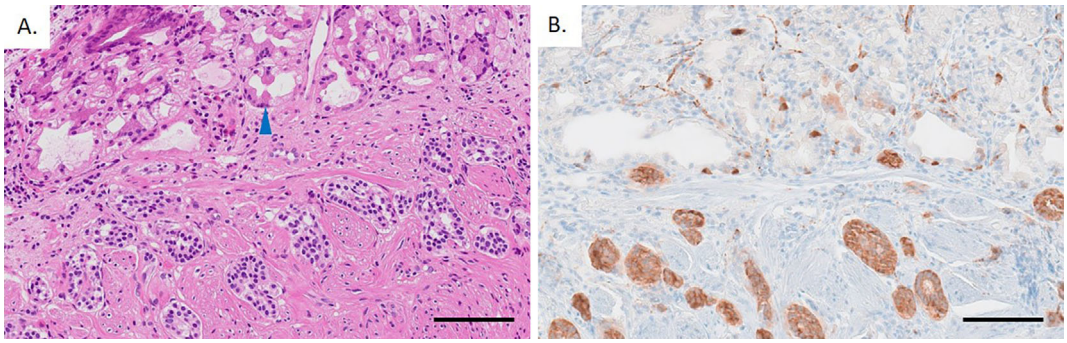

Figure 6. **Histopathological findings of ECL cell hyperplasia/dysplasia. Small nodules of ECL cells <500 μm in diameter were found around the muscularis mucosa on Hematoxylin and Eosin staining (A) and synaptophysin staining (B), which was diagnosed as ECL cell hyperplasia/dysplasia. In the subclassification of ECL cell hyperplasia/dysplasia, these nodules were diagnosed as micronodular hyperplasia because the size of each nodule was <150 μm. Parietal cell protrusion was also found (A, blue arrow). ECL: enterochromaffin-like**

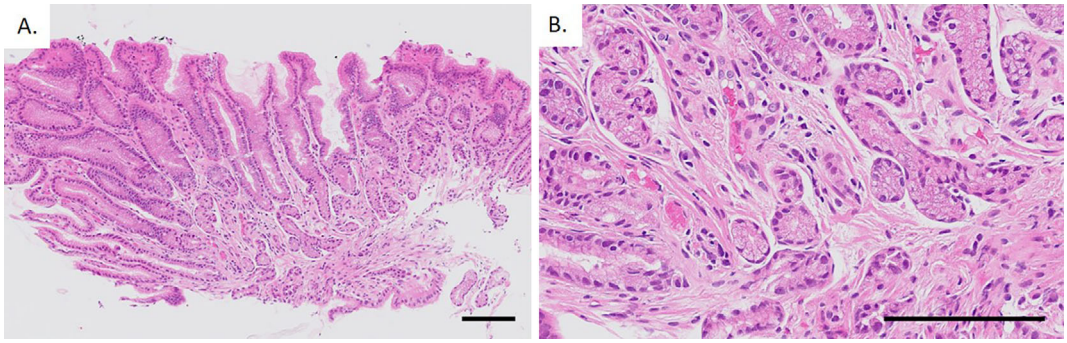

Figure 7. **Histopathological findings of antral mucosa. An endoscopic biopsy of the endoscopically non-NEN antral mucosa showed no intestinal metaplasia and the presence of pyloric glands (A, B). NEN: neuroendocrine neoplasm**

Table 2. Reports of Gastric NENs with Parietal Cell Dysfunction.

References	Age (y)/ sex	Diameter and number of tumors	Endoscopic findings of background gastric mucosa in C-WLI	Serum gastrin level (pg/mL)	Autoantibody	Hematoxylin and Eosin staining for parietal cells	Immunostaining of H^+K^+-ATPase	Treatment, clinical outcome
9	37/male	<5 mm, >20	No atrophy	6,800	PCA, normal; IFA, negative	Parietal cell protrusion, vacuolation, dilated fundic glands	Completely negative for α and β subunits	Observation
9	36/male	Small, multiple	No atrophy	2,600	PCA, normal; IFA, negative	Parietal cell protrusion, vacuolation, dilated fundic glands	Completely negative for α and β subunits	Anterectomy
13	47/male	6-15 mm, 19	No atrophy	>800	PCA, normal; IFA, negative	Dilated fundic glands, hypertrophy and hyperplasia of parietal cells	NA	Proximal gastrectomy, with lymphadenectomy, no metastasis
14	54/male	1-13 mm, >10	Thickened gastric folds	1,400	PCA, normal	Dilated oxyntic glands, hypertrophy and hyperplasia of parietal cells	Weak stain for β subunit	Subtotal gastrectomy with anterectomy, Positive for LN metastasis
15	50/female	2-12 mm, multiple	No atrophy	1,400	PCA, normal	Vacuolation, dilated oxyntic glands, hypertrophy and hyperplasia of parietal cells	NA	Total gastrectomy with lymphadenectomy, no metastasis
Present case	69/female	<5 mm, 6	Discolored mucosa with marked vascular visibility in the corpus	11,675	PCA, normal; IFA, negative	Parietal cell protrusion, vacuolation, dilated fundic glands	Completely negative	Observation

NENs: neuroendocrine neoplasms, C-WLI: conventional white light imaging, PCA: parietal cell antibody, IFA: intrinsic factor antibody, NA: no assessment, LN: lymph node

This type of NEN cannot be subdivided into the traditional three types of NENs because these tumors showed hypergastrinemia and achlorhydria with neither chronic atrophic gastritis nor MEN-1 in the underlying disease. However, NENs with parietal cell dysfunction are a type of ECL-cell NEN, and the mechanism underlying the incidence of such NENs is similar to that of type I gastric NENs. In either type of NEN, dysfunction or depletion of parietal cells causes achlorhydria, hypergastrinemia due to G cell hyperplasia, ECL cell hyperplasia and finally NENs (9). Although the prognosis of NENs with parietal cell dysfunction is unclear, the mechanism of incidence might indicate a relatively good prognosis, similar to that of type I gastric NEN.

The diagnostic criteria for autoimmune gastritis have not been established, but the presence of parietal cell antibody and intrinsic factor antibody-negative cases has been reported (17). In the present case, NENs due to autoantibody-negative autoimmune gastritis and parietal cell dysfunction were considered as differential diagnoses. Although parietal cell dysfunction showed no atrophic change in the background gastric mucosa in the previous cases (9, 15), severe atrophic changes in the corpus were suspected in C-WLI because the endoscopic findings met the criteria for severe atrophic gastritis (18). In contrast, ME-NBI revealed a slightly enlarged, round pit with unclear or irregular subepithelial capillary networks, which indicates only mild gastritis according to the classification proposed by Tahara et al. (3). Among cases with this ME-NBI finding, 85.7% were reported to lack severe gastric atrophy by histopathology (19). Indeed, the present case also showed very mild inflammation in the histopathology. The reason for the discrepancy in gastric atrophy between C-WLI and ME-NBI or histopathological findings is unclear; however, vacuolated parietal cell cytoplasm might be associated with a thin, discolored mucosa with marked vascular visibility on C-WLI. In this regard, the ME-NBI findings might help differentiate parietal cell dysfunction from autoantibody-negative autoimmune gastritis other than the early type, as described below.

ME-NBI showed an absent microsurface pattern on the top of the gastric NEN, which reflects the fact that this tumor grew beneath the epithelium without a gland structure. This ME-NBI finding is in accordance with the characteristics described in a previous report about gastric NEN (20). Regarding the histopathology of the biopsy specimen, the tumor was located beneath a monolayer of foveolar epithelium. Tumors without a gland structure, such as lymphoma and poorly differentiated cancer covered with a thin normal gastric layer, often have an absent microsurface pattern on ME-NBI, and this was also true in the present case.

This case showed an extremely high serum gastrin level (11,675 pg/mL). Previous studies defined values exceeding 300-450 pg/mL as indicating the presence of hypergastrine-

Table 3. Comparison of Characteristics between Parietal Cell Dysfunction and Early-stage Autoimmune Gastritis.

	Parietal cell dysfunction	Early-stage autoimmune gastritis
Endoscopic finding in corpus	• No atrophy	• Polygonal areae gastricae surrounded by a reticular border in a mosaic-like pattern
	• Thickened gastric folds	• Edematous mucosa and slight swelling of the areae gastricae
	• Discolored mucosa with marked vascular visibility	• Discolored mucosa and vascular visibility
		• Reddish and edematous change of the gastric areas
		• No significant atrophic change
Hematoxylin and Eosin staining in corpus	• Parietal cell protrusion	• Parietal cell protrusion
	• Parietal cell vacuolation	• Parietal cell vacuolation
	• Dilated fundic glands	• Dilated fundic glands
		• Inflammation in deep mucosa
		• Reduction of parietal cells
Immunostaining for H^+K^+-ATPase	• Negative (or weak)	• Negative or weak in some areas
Immunostaining for pepsinogen	• Positive	• Negative or weak in some areas
Autoantibody	• PCA, normal	• PCA, high (possibly normal in some cases)
	• IFA, negative	• IFA, positive or negative

PCA: parietal cell antibody, IFA: intrinsic factor antibody

mia in gastric NENs (21, 22). Among gastric NENs with hypergastrinemia, the serum gastrin levels in cases with parietal cell dysfunction were reported to be 1,400-6,800 pg/mL, and those in some patients with type I NENs were >10,000 pg/mL (21). Although some clinicians believe such high levels of serum gastrin occur frequently in patients with Zollinger-Ellison syndrome (ZES), including MEN-1 (23), this was not the case. Indeed, serum gastrin levels >10,000 pg/mL are also uncommon in patients with ZES, occurring in 4.9-9% of such patients (23). Thus, although the presence/absence of hypergastrinemia is useful for distinguishing type III from type I, type II, or parietal cell dysfunction in gastric NENs, it may be difficult to distinguish the latter three types of gastric NENs by the serum gastrin level alone.

This case has some limitations in its applicability to the diagnosis of parietal cell dysfunction. First, although we confirmed a lack of H^+K^+-ATPase expression on immunostaining, other functions, such as the intrinsic factor production, were unknown. However, to our knowledge, there are no other immunostaining approaches that can evaluate the parietal cell function. Second, early-stage autoimmune gastritis cannot be ruled out. Recently, several cases of early-stage autoimmune gastritis have been reported, and several histopathological findings, such as parietal cell protrusion, dilated fundic glands and a lack of H^+K^+-ATPase expression, were also found in these cases (24-26). Although the parietal cell autoantibody titer was normal in the present case, differing from the previous cases (24-26), autoantibody-negative early-stage autoimmune gastritis could not be ruled out. Considering the similar histopathological findings between parietal cell dysfunction and early-stage autoimmune gastritis (Table 3), we hypothesize that parietal cell dysfunction and autoantibody-negative early-stage autoimmune gastritis are similar diseases. However, to confirm this hypothesis, long-term observation to evaluate whether or not the corporal gastritis is progressing is required.

In conclusion, we experienced a rare case of multiple NENs with parietal cell dysfunction that had extreme hypergastrinemia. When we encounter patients with multiple gastric NENs with achlorhydria and hypergastrinemia, parietal cell dysfunction should be considered as a differential diagnosis. ME-NBI may help lead to the diagnosis of such a disease, and a subsequent histopathological evaluation of the fundic gland mucosa is required.

The authors state that they have no Conflict of Interest (COI).

References

1. Rindi G, Luinetti O, Cornaggia M, et al. Three subtypes of gastric argyrophil carcinoid and the gastric neuroendocrine carcinoma: a clinicopathologic study. Gastroenterology **104**: 994-1006, 1993.
2. Delle Fave G, O'Toole D, Sundin A, et al. ENETS consensus guidelines update for gastroduodenal neuroendocrine neoplasms. Neuroendocrinology **103**: 119-124, 2016.
3. Tahara T, Shibata T, Nakamura M, et al. Gastric mucosal pattern by using magnifying narrow-band imaging endoscopy clearly distinguishes histological and serological severity of chronic gastritis. Gastrointest Endosc **70**: 246-253, 2009.
4. Bansal A, Ulusarac O, Mathur S, et al. Correlation between narrow band imaging and nonneoplastic gastric pathology: a pilot feasibility trial. Gastrointest Endosc **67**: 210-216, 2008.
5. Iijima K, Ohara S, Sekine H, et al. A new endoscopic method of gastric acid secretory testing. Am J Gastroenterol **93**: 2113-2118, 1998.
6. Hatta W, Iijima K, Koike T, et al. Endoscopic findings for predicting gastric acid secretion status. Dig Endosc **27**: 582-589, 2015.
7. Kikuchi H, Fukuda S, Koike T, et al. Association of residual gastric acid secretion with persistent symptoms in gastroesophageal reflux disease patients receiving standard-dose proton pump inhibitor therapy. Esophagus **18**: 380-387, 2021.
8. Solcia E, Bordi C, Creutzfeldt W, et al. Histopathological classifi-

cation of nonantral gastric endocrine growths in man. Digestion **41**: 185-200, 1988.
9. Ishioka M, Hirasawa T, Kawachi H, et al. Enterochromaffin-like cell neuroendocrine tumor associated with parietal cell dysfunction. Gastrointest Endosc **90**: 841-845 e1, 2019.
10. Modlin IM, Lye KD, Kidd M. A 50-year analysis of 562 gastric carcinoids: small tumor or larger problem? Am J Gastroenterol **99**: 23-32, 2004.
11. Niederle MB, Hackl M, Kaserer K, et al. Gastroenteropancreatic neuroendocrine tumours: the current incidence and staging based on the WHO and European Neuroendocrine Tumour Society classification: an analysis based on prospectively collected parameters. Endocr Relat Cancer **17**: 909-918, 2010.
12. O'Connor JM, Marmissolle F, Bestani C, et al. Observational study of patients with gastroenteropancreatic and bronchial neuroendocrine tumors in Argentina: results from the large database of a multidisciplinary group clinical multicenter study. Mol Clin Oncol **2**: 673-684, 2014.
13. Ooi A, Ota M, Katsuda S, et al. An unusual case of multiple gastric carcinoids associated with diffuse endocrine cell hyperplasia and parietal cell hypertrophy. Endocr Pathol **6**: 229-237, 1995.
14. Abraham SC, Carney JA, Ooi A, et al. Achlorhydria, parietal cell hyperplasia, and multiple gastric carcinoids: a new disorder. Am J Surg Pathol **29**: 969-975, 2005.
15. Nakata K, Aishima S, Ichimiya H, et al. Unusual multiple gastric carcinoids with hypergastrinemia: report of a case. Surg Today **40**: 267-271, 2010.
16. Rahman MA, Karam SM. Gastric parietal cell vacuolation mimicking gastric carcinoma. Histopathology **63**: 735-737, 2013.
17. Lahner E, Norman GL, Severi C, et al. Reassessment of intrinsic factor and parietal cell autoantibodies in atrophic gastritis with respect to cobalamin deficiency. Am J Gastroenterol **104**: 2071-2079, 2009.
18. Kimura K. Chronological transition of the fundic-pyloric border determined by stepwise biopsy of the lesser and greater curvatures of the stomach. Gastroenterology **63**: 584-592, 1972.
19. Tahara T, Shibata T, Nakamura M, et al. Gastric mucosal pattern by using magnifying narrow-band imaging endoscopy clearly distinguishes histological and serological severity of chronic gastritis. Gastrointest Endosc **70**: 246-253, 2009.
20. Sato Y. Endoscopic diagnosis and management of type I neuroendocrine tumors. World J Gastrointest Endosc **7**: 346-353, 2015.
21. Sato Y, Imamura H, Kaizaki Y, et al. Management and clinical outcomes of type I gastric carcinoid patients: retrospective, multicenter study in Japan. Dig Endosc **26**: 377-384, 2014.
22. Vanoli A, La Rosa S, Miceli E, et al. Prognostic evaluations tailored to specific gastric neuroendocrine neoplasms: analysis of 200 cases with extended follow-up. Neuroendocrinology **107**: 114-126, 2018.
23. Berna MJ, Hoffmann KM, Serrano J, et al. Serum gastrin in Zollinger-Ellison syndrome: I. prospective study of fasting serum gastrin in 309 patients from the National Institutes of Health and comparison with 2229 cases from the literature. Medicine (Baltimore) **85**: 295-330, 2006.
24. Kotera T, Oe K, Kushima R, et al. Multiple pseudopolyps presenting as reddish nodules are a characteristic endoscopic finding in patients with early-stage autoimmune gastritis. Intern Med **59**: 2995-3000, 2020.
25. Ayaki M, Aoki R, Matsunaga T, et al. Endoscopic and upper gastrointestinal barium X-ray radiography images of early-stage autoimmune gastritis: a report of two cases. Intern Med **60**: 1691-1696, 2021.
26. Kishino M, Yao K, Hashimoto H, et al. A case of early autoimmune gastritis with characteristic endoscopic findings. Clin J Gastroenterol **14**: 718-724, 2021.